

## Loss-of-Function Mutations in *SERPINB8* Linked to Exfoliative Ichthyosis with Impaired Mechanical Stability of Intercellular Adhesions

Manuela Pigors,<sup>1</sup> Ofer Sarig,<sup>2</sup> Lisa Heinz,<sup>3</sup> Vincent Plagnol,<sup>4</sup> Judith Fischer,<sup>3</sup> Janan Mohamad,<sup>2</sup> Natalia Malchin,<sup>2</sup> Shefali Rajpopat,<sup>1</sup> Monia Kharfi,<sup>5</sup> Giles G. Lestringant,<sup>6</sup> Eli Sprecher,<sup>2</sup> David P. Kelsell,<sup>1,7,\*</sup> and Diana C. Blydon<sup>1,7,\*</sup>

SERPINS comprise a large and functionally diverse family of serine protease inhibitors. Here, we report three unrelated families with loss-of-function mutations in *SERPINB8* in association with an autosomal-recessive form of exfoliative ichthyosis. Whole-exome sequencing of affected individuals from a consanguineous Tunisian family and a large Israeli family revealed a homozygous frameshift mutation, c.947delA (p.Lys316Serfs\*90), and a nonsense mutation, c.850C>T (p.Arg284\*), respectively. These two mutations are located in the last exon of *SERPINB8* and, hence, would not be expected to lead to nonsense-mediated decay of the mRNA; nonetheless, both mutations are predicted to lead to loss of the reactive site loop of SERPINB8, which is crucial for forming the SERPINB8-protease complex. Using Sanger sequencing, a homozygous missense mutation, c.2T>C (p.Met1?), predicted to result in an N-terminal truncated protein, was identified in an additional family from UAE. Histological analysis of a skin biopsy from an individual homozygous for the variant p.Arg284\* showed disadhesion of keratinocytes in the lower epidermal layers plus decreased SERPINB8 levels compared to control. In vitro studies utilizing siRNA-mediated knockdown of *SERPINB8* in keratinocytes demonstrated that in the absence of the protein, there is a cell-cell adhesion defect, particularly when cells are subjected to mechanical stress. In addition, immunoblotting and immunostaining revealed an upregulation of desmosomal proteins. In conclusion, we report mutations in *SERPINB8* that are associated with exfoliative ichthyosis and provide evidence that SERPINB8 contributes to the mechanical stability of intercellular adhesions in the epidermis.

Rare genodermatoses with underlying mutations in genes encoding for proteases and protease inhibitors demonstrate that a dynamic balance between the activities of proteases and their inhibitors is indispensable for maintaining epidermal homeostasis.<sup>1,2</sup> One such class of inhibitors is the SERPIN family of serine peptidase inhibitors. Mutations in *SERPINB7* (MIM: 603357) were identified in individuals with Nagashima-type palmoplantar keratosis (MIM: 615598)<sup>3,4</sup> and genome-wide association studies have linked the *SERPINB8* (MIM: 601697) locus with psoriasis.<sup>5</sup> Furthermore, *SERPINB3* (MIM: 600517), *SERPINB4* (MIM: 600518), and *SERPINB13* (MIM: 604445) have also been recently linked to psoriasis (MIM: 177900) and atopic eczema (MIM: 605803) via transcriptomic and proteomic approaches.<sup>1</sup> Serine protease cascades appear to be involved in various processes that are essential for epidermal differentiation, such as lipid barrier formation and assembly of the cornified envelope.<sup>6</sup> In this study, we report three families with putative loss-of-function mutations in the serpin peptidase inhibitor, clade B, member 8—*SERPINB8*—linked to autosomal-recessive exfoliative ichthyosis. In vivo and in vitro studies demonstrate that loss of SERPINB8 impairs keratinocyte mechanical stability.

Family 1 was from Tunisia and a history of parental relatedness was present. The index individual, a 5-year-old boy,

suffered since he was 3 months old from superficial peeling of small areas of the palmar and dorsal faces of his hands and feet, painless and easily removed, with an underlying erythema. The symptoms were aggravated by heat, humidity, and friction (Figure 1A). His 3-year-old sister had the same symptoms.

An additional individual from a second family from the United Arab Emirates was ascertained. She presented with a similar clinical phenotype as the two affected individuals of family 1 but peeling was present also on her lower arms (Figure 1B).

The third family enrolled in this study originated from Israel and was of Jewish Ashkenazi extraction. All three affected individuals presented with a more severe peeling compared to the affected individuals of families 1 and 2. Age of onset was between 4 and 6 months. Clinical examination revealed superficial white scale with no significant erythema over their lower extremities and diffuse yellowish hyperkeratotic plaques over the palms and soles (Figures 1C–1E). In contrast to individuals with Nagashima-type palmoplantar keratosis caused by mutations in *SERPINB7*, no whitish change upon water exposure was observed on hyperkeratotic palms of affected individuals of family 3. Of note, the maternal grandfather and his sister were affected by psoriasis.

<sup>1</sup>Centre for Cell Biology and Cutaneous Research, Blizard Institute, Barts and the London School of Medicine and Dentistry, Queen Mary University of London, London E1 2AT, UK; <sup>2</sup>Department of Dermatology, Tel Aviv Sourasky Medical Center, 64239 Tel Aviv, Israel; <sup>3</sup>Institute of Human Genetics, University Medical Center Freiburg, 79106 Freiburg, Germany; <sup>4</sup>University College London Genetics Institute, London WC1E 6BT, UK; <sup>5</sup>Department of Dermatology, Charles Nicolle Hospital, 1006 Tunis, Tunisia; <sup>6</sup>Consultant Dermatologist (retired), British Ministry of Defence, London SW1A 2HB, UK

<sup>7</sup>These authors contributed equally to this work and are joint senior authors

\*Correspondence: [d.p.kelsell@qmul.ac.uk](mailto:d.p.kelsell@qmul.ac.uk) (D.P.K.), [d.blydon@qmul.ac.uk](mailto:d.blydon@qmul.ac.uk) (D.C.B.)

<http://dx.doi.org/10.1016/j.ajhg.2016.06.004>

© 2016 American Society of Human Genetics.

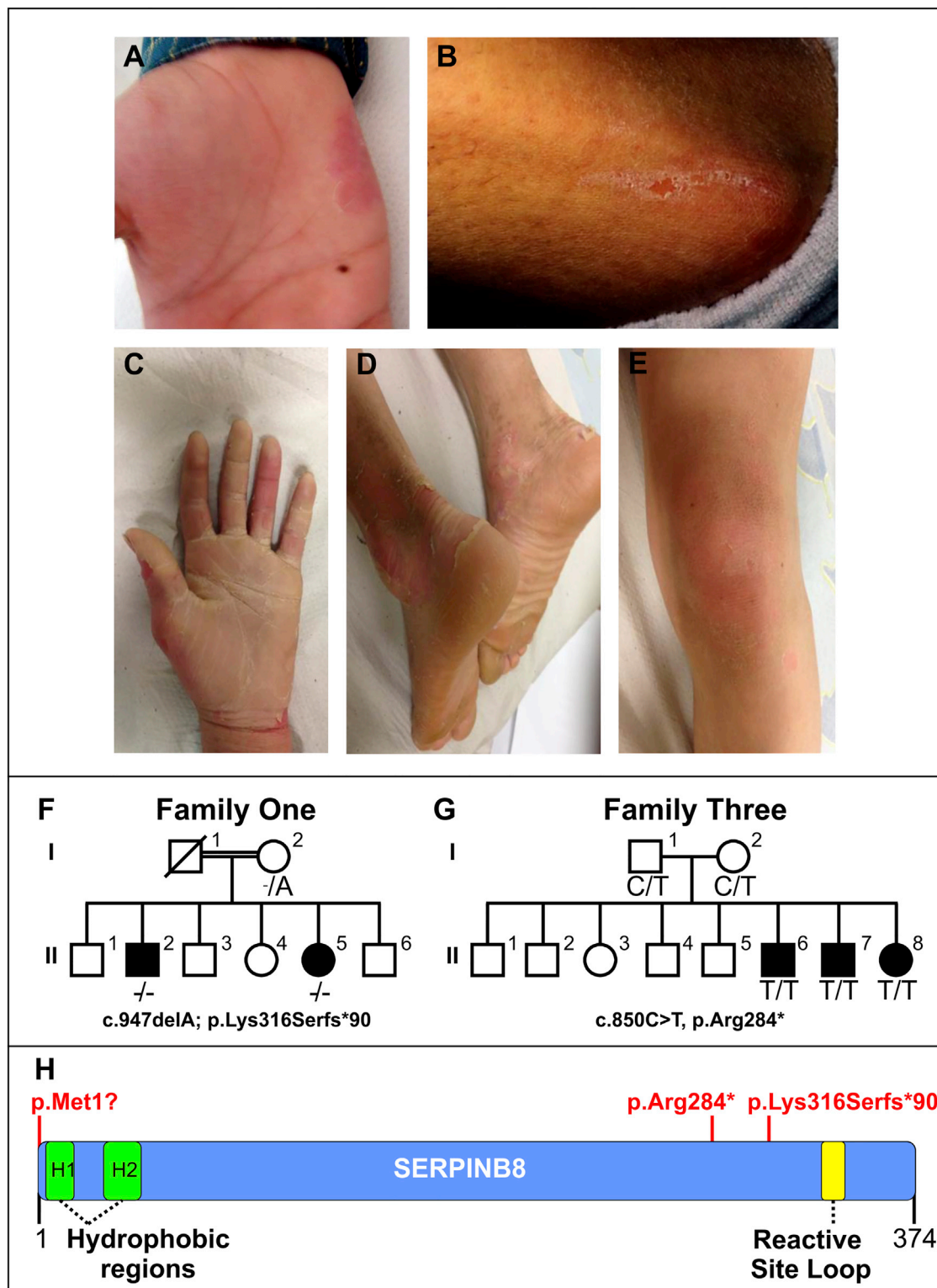


**Figure 1. Clinical Features, Pedigrees, and *SERPINB8* Mutations of Individuals with Autosomal-Recessive Exfoliative Ichthyosis**  
 (A) Individual II-2 from family 1 showed superficial peeling of small areas of his palmar surfaces, with an underlying erythema.  
 (B) The only affected individual of family 2 presented with a mild peeling on her forearms.  
 (C and D) Diffuse yellowish hyperkeratotic plaques on the palms and soles of individuals II-7 (C) and II-8 (D) of family 3.  
 (E) Individual II-8 of family 3 displayed superficial white scale with no significant erythema over her lower extremities.  
 (F and G) Pedigrees and genotypes of families 1 and 3. The homozygous frameshift variant c.947delA (p.Lys316Serfs\*90) was identified in individuals II-2 and II-5 of family 1, who were born to consanguineous parents (F). The homozygous nonsense mutation c.850C>T (p.Arg284\*) in *SERPINB8* was identified in individuals II-6, II-7, and II-8 of family 3 (G).

(legend continued on next page)

After obtaining written informed consent, genomic DNA was extracted from EDTA-blood samples from all affected individuals and available family members. The project was approved by the East London and City Health Authority Research Ethics Committee and was conducted according to the Declaration of Helsinki Principles. Initially, high-resolution homozygosity mapping was performed by genotyping both affected individuals, II-2 and II-5, of family 1 using the Affymetrix GeneChip Human Mapping 250K Nsp SNP array. Analysis was performed as described<sup>7</sup> and a large block of 98.6% homozygosity shared by both siblings was identified on chromosome 18 between rs1944983 and rs2194631, which contains several SERPIN genes. Subsequently, DNA samples from both affected siblings of family 1 were subjected to whole-exome sequencing. Genomic DNA was extracted from EDTA blood using the QiAmp DNA Mini Kit (QIAGEN). Exome sequencing was performed with 3 µg of genomic DNA. Exome capture and enrichment was performed with the NimbleGen SeqCap EZ Library protocol (Roche Nimblegen). The subsequent DNA library was sequenced on an Illumina HiSeq2000. Variants were filtered against dbSNP137, the 1000 Genomes Project, and HapMap8, as described previously.<sup>8</sup> Given the parental relatedness of family 1, we assumed that the peeling skin disorder is inherited in an autosomal-recessive manner and so the underlying gene mutation was expected to be homozygous in the two siblings. In a region of homozygosity located on chromosome 18, the frameshift mutation in *SERPINB8*, exon 7 (c.947delA [p.Lys316Serfs\*90]), was identified in both individuals and confirmed by Sanger sequencing (Figure 1F). The mother was heterozygous for the deletion. No DNA was available from the father. Unaffected siblings were either heterozygous for the frameshift variant or wild-type, supporting an autosomal-recessive mode of disease transmission. The deletion mutation is located a few base pairs upstream of the sequence that encodes for the reactive site loop (Figure 1H), which is crucial for binding of SERPINB8 to its target protease.<sup>9,10</sup> Because the deletion is located in exon 7 (the last exon) of *SERPINB8* and leads to a frameshift, we predict that the transcript will not be subjected to nonsense-mediated mRNA decay, but rather the mutation results in a C-terminally extended SERPINB8 peptide that lacks the reactive site loop. The frameshift variant was also disclosed in a homozygous state in two individuals and in a heterozygous state in six individuals of the putative healthy control population with a minor allele frequency of 0.079% (Exome Variant Server). There have been no reports of individuals homozygous for the frameshift variant in dbSNP, 1000 Genomes, and ExAC Browser.

However, we argue that due to the mild phenotype, some affected individuals can easily go undiagnosed.

In order to verify that mutations in *SERPINB8* underlie the exfoliative ichthyosis, ten individuals with similar clinical pictures were screened for *SERPINB8* mutations via Sanger sequencing. Exon/intron boundaries of *SERPINB8* were amplified by PCR with primers designed with Primer3 Software (v.0.4.0). Primer sequences are listed in Table S1. DNA sequencing was done using BigDye terminator master mix (ThermoFisher) and generated sequences were aligned and compared with the reference sequence from NCBI Entrez Nucleotide database (GenBank: NM\_198833) using the web-based program MultAlin. A homozygous missense mutation in *SERPINB8*, exon 2 (c.2T>C [p.Met1?]), was identified in the affected individual of family 2 (Figure 1H). The mother was heterozygous for the missense mutation. No DNA was available from the father to perform carrier testing. The mutation was predicted to be probably damaging by PolyPhen-2 with a score of 1 and disease-causing by MutationTaster with a score of 1. It affects the start codon of the longest *SERPINB8* transcript, isoform a (GenBank: NM\_198833.1), and interferes with initiation of translation, putatively giving rise to an N-terminal truncated SERPINB8. NCBI ORF Finder software identified an alternative in-frame start codon, 33 codons downstream of the initial start codon. Moreover, a shorter isoform c of *SERPINB8* exists (GenBank: NM\_001276490.1), which uses an alternate splice junction in the 5' UTR and lacks the first exon containing the translation start site compared to isoform a and, therefore, translation of isoform c is not affected.

Subsequently, exome sequencing in individuals II-6 and I-2 of a large Israeli family (family 3) was performed (Figure 1G). Genomic DNA was extracted from peripheral blood leukocytes using the 5 Prime ArchivePure DNA Blood Kit (5 Prime Inc.). Exome sequencing was performed by BGI Tech Solutions Ltd. Whole-exome capture was carried out by in-solution hybridization with SureSelect All Exon 51Mb v.4.0 (Agilent) followed by massively parallel sequencing (Illumina HiSeq2000) with 100-bp paired-end reads. Reads were aligned to the Genome Reference Consortium Human Build 37 (GRCh37/hg19) using Burrows-Wheeler Aligner.<sup>11</sup> Duplicate reads, resulting from PCR clonality or optical duplicates, and reads mapping to multiple locations were excluded from downstream analysis. Reads mapping to a region of known or detected insertions or deletions were re-aligned to minimize alignment errors. Single-nucleotide substitutions and small insertion deletions were identified and quality filtered with the Genome Analysis Tool Kit.<sup>12</sup> Rare variants were identified by filtering using the data from dbSNP138, the 1000 Genomes

---

(H) Schematic representation of SERPINB8 and its domains. SERPINB8 contains two hydrophobic regions (H1 and H2), which are thought to be important for secretion of the protein, and a reactive site loop (RSL), which is crucial for its interaction with target substrates. The mutations are indicated in red. The variant p.Met1? affects the start codon, predicted to result in an N-terminal truncated protein lacking both hydrophobic regions. p.Lys316Serfs\*90 and p.Arg284\* are located a few amino acids upstream of the RSL and are predicted to lead to loss of the RSL.

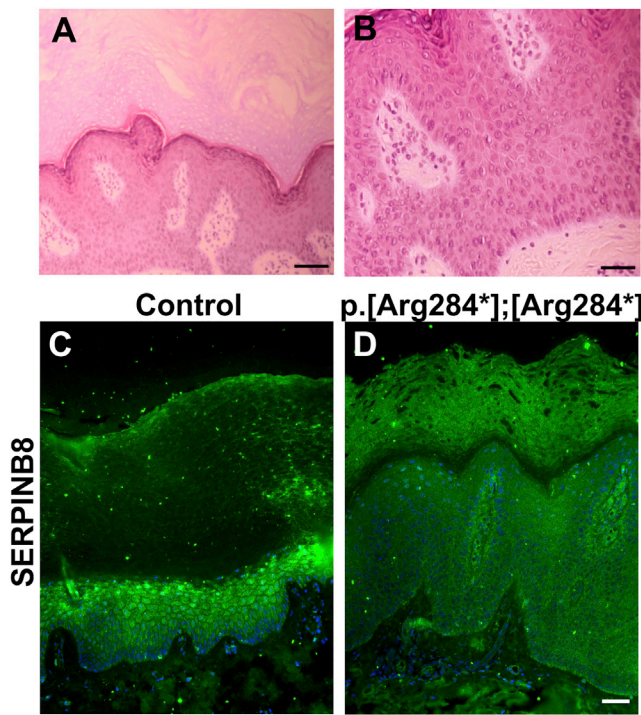


**Figure 2. Morphological Analysis of SERPINB8 Loss-of-Function Skin**

(A and B) Skin biopsies obtained from individual II-6 of family 3 demonstrated acanthosis, hyperkeratosis, and disadhesion of keratinocytes in the basal and suprabasal layers of the epidermis with evidence of intercellular space widening. (Hematoxylin and eosin; scale bars represent 100  $\mu\text{m}$  in A and 40  $\mu\text{m}$  in B.)

(C and D) Indirect immunofluorescence analysis of SERPINB8 in control and SERPINB8 loss-of-function skin. The monoclonal anti-SERPINB8 antibody (Santa Cruz cat# sc-101371; RRID: AB\_2186486) showed a cytoplasmic and nuclear distribution of the protease inhibitor in the suprabasal and granular layers in control skin (C). SERPINB8 signals were strongly reduced in the skin of the individual homozygous for p.Arg284\* (D). Scale bar represents 200  $\mu\text{m}$ .

Project, the Exome Variant Server, and an in-house database of sequenced individuals. Variants were classified by predicted protein effects using PolyPhen-2 and SIFT.<sup>13,14</sup> The homozygous nonsense mutation c.850C>T (p.Arg284\*) in exon 7 in *SERPINB8* was identified in individual II-6 (Figures 1G and 1H). His mother was heterozygous carrier of the mutation. Sanger sequencing was performed in all other available family members. Both affected siblings, II-7 and II-8, were also found to be homozygous for p.Arg284\*. The father was confirmed to be heterozygous carrier of the mutation together with four healthy siblings (Figure 1G). A skin biopsy was obtained from individual II-6 of family 3 and H&E staining revealed acanthosis, hyperkeratosis, and disadhesion of keratinocytes in the basal and suprabasal layers of the epidermis with evidence of intercellular space widening (Figures 2A and 2B). In addition, indirect immunofluorescence analysis was performed in paraffin-embedded sections of palmar skin of individual II-6 and compared to a matched control subject. Localization of SERPINB8 was assessed

with the monoclonal anti-SERPINB8 antibody (Santa Cruz cat# sc-101371; RRID: AB\_2186486), which showed a cytoplasmic and nuclear distribution mainly in the suprabasal and granular layers of control skin (Figure 2C). SERPINB8 was strongly reduced in the proband's skin (Figure 2D).

In order to further characterize the loss of SERPINB8 in keratinocytes, we utilized a siRNA pool to knockdown SERPINB8 in the HaCaT human keratinocyte cell line. ON-TARGETplus SMART-pool siRNA (Dharmacon) was used to knock down SERPINB8 in the HaCaT cells. Control keratinocytes were treated with a non-targeting pool (NTP) (Dharmacon). 72 hr after transfection, the efficiency of the knockdown was validated by immunoblotting with a primary antibody against SERPINB8 (Santa Cruz) (Figure 3A). Because the symptoms in all affected individuals mainly occurred on sites exposed to high mechanical trauma, we first studied the effect of mechanical stress on keratinocytes by means of a disperse-based dissociation assay. In this assay, relative changes in epithelial cohesion were monitored by comparing the number of fragments in control and knockdown (KD) cells after treatment with disperse. Cystatin A (*CSTA*)-KD cells were used as positive control because we have previously shown that loss of this protease inhibitor impairs cell-cell adhesion.<sup>7</sup> The disperse-based dissociation assay was performed as described elsewhere.<sup>15</sup> In brief, 72 hr after transfection of HaCaT cells with NTP, *CSTA* siRNA, or *SERPINB8* siRNA, confluent cell monolayers were treated with 700  $\mu\text{L}$  of 5 mg/mL disperse for approximately 30 min at 37°C until the monolayers were detached completely. Released monolayers were washed twice in 500  $\mu\text{L}$  PBS, transferred to 2 mL tubes, and subjected to 50 inversion cycles. The fragments were counted under an inverted microscope. Similar to *CSTA*, *SERPINB8*-KD cells showed an increased number of fragments compared to the NTP control cells, indicating that cell-cell adhesion is impaired in both *CSTA*-KD and *SERPINB8*-KD cells (Figure 3B). The desmosomes represent one of the major intercellular adhesive junctions in the epidermis, so we assessed the protein levels of two desmosomal molecules, desmoplakin (DP-1, Progen) and desmoglein-1 (clone MCA2271, Bio-Rad AbD). Immunoblotting showed an upregulation of both desmosomal proteins in the *SERPINB8*-KD cells, compared to NTP control cells (Figure 3C). In addition, keratinocyte monolayers were exposed to oscillating mechanical stress using the Flexcell FX-4000 tension system (Flexcell International). The stretching assay was performed as described previously.<sup>7</sup> In brief, HaCaT cells were seeded on BioFlex 6-well plates coated with pronectin (Flexcell International). 72 hr after transfection of HaCaT cells with NTP or *SERPINB8* siRNA, monolayers were subjected to cyclic mechanical stress for 4 hr with a frequency of 5 Hz and an elongation of amplitude ranging from 10% to 13%. A FlexStop valved rubber stopper was used to prevent control (non-stretched, 0 hr) cells from being exposed to mechanical loads. The efficiency of the KD of SERPINB8 was validated by

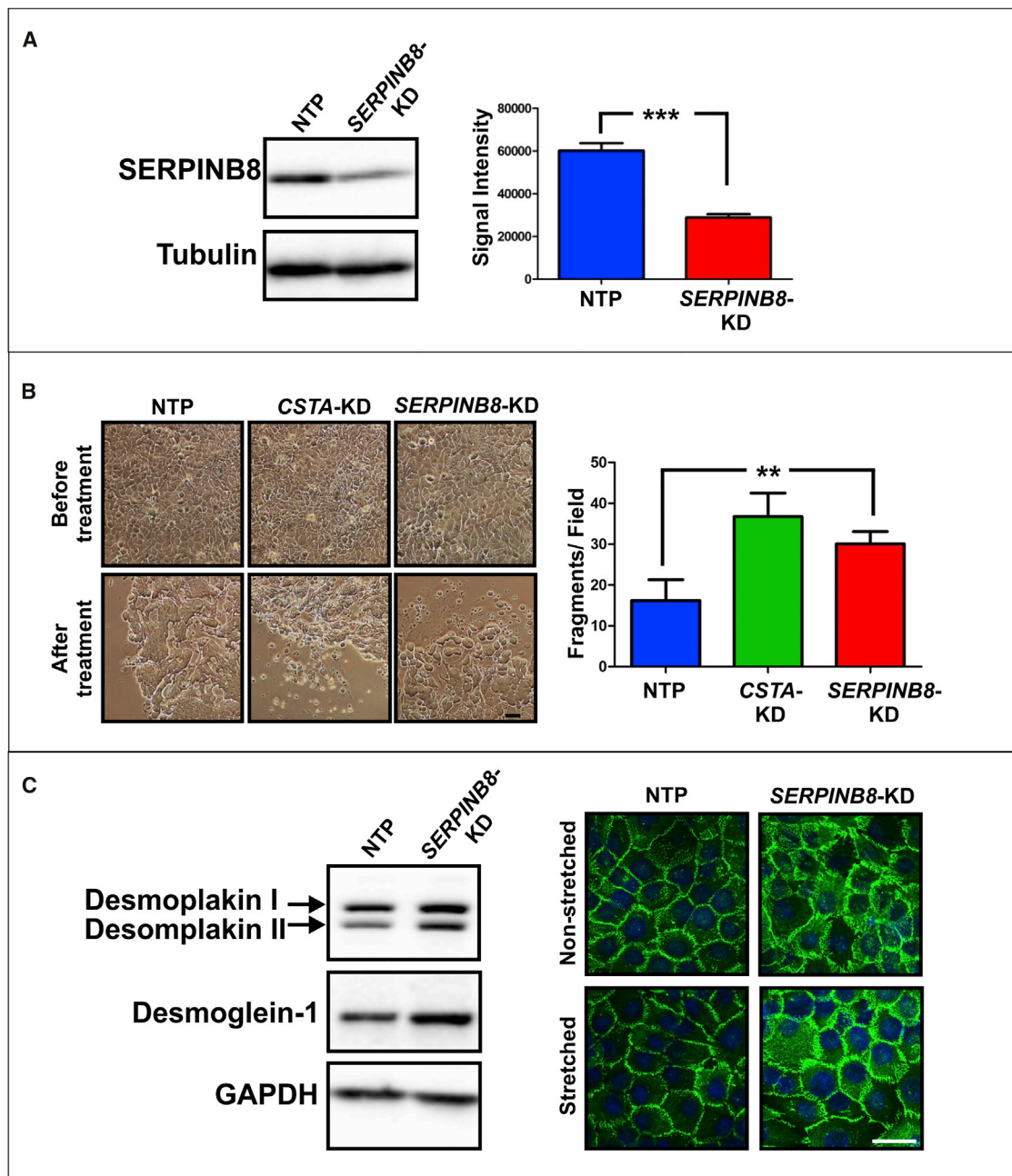


### Figure 3. Knockdown of SERPINB8 Affects Cell-Cell Adhesion In Vitro

(A) A siRNA pool was utilized to knockdown SERPINB8 in HaCaT cells. SERPINB8 protein levels were compared to control cells treated with a non-targeting pool (NTP) and the efficiency of the KD was validated by immunoblotting (data represent mean  $\pm$  SEM, \*\*\* $p \leq 0.001$ , Student's t test).

(B) A disperse-based dissociation assay was performed to assess intercellular adhesion by the degree of cell monolayer integrity upon mechanical stress. Similar to Cystatin A (CSTA)-KD, SERPINB8-KD cells showed an increased number of fragments compared to NTP control cells (data represent mean  $\pm$  SEM, \*\* $p \leq 0.01$ , Student's t test). Scale bar represents 50  $\mu$ m.

(C) Immunoblotting of cell lysates from SERPINB8-KD cells showed an upregulation of both desmoplakin isoforms I and II as well as increased levels of desmoglein-1, as compared to NTP control cells. Likewise, immunostaining revealed a strong upregulation of desmoplakin in SERPINB8-KD cells. Upon stretching of SERPINB8-KD monolayers for 4 hr, desmoplakin levels were even more prominent in the SERPINB8-KD cells. Scale bar represents 40  $\mu$ m.

immunoblotting and quantitative real-time PCR (qPCR) (Figure S1). No morphological changes were observed, but indirect immunofluorescence staining revealed increased levels of desmoplakin (DP-1, Progen) along the plasma membrane in both stretched and non-stretched

SERPINB8-KD keratinocytes, with stretched SERPINB8-KD cells showing a more striking increase in desmoplakin levels, compared to NTP control cells (Figure 3C). Moreover, the desmoplakin staining pattern showed evidence of a shift from a plasma membranous localization in NTP

control cells to increased cytoplasmic localization in *SERPINB8*-KD cells (Figure 3C). qPCR data shows that the mRNA levels of desmoplakin isoforms I and II and desmoglein-1 were decreased in *SERPINB8*-KD cells indicating that the increased protein levels observed for these desmosomal proteins is not due to an upregulation of mRNA transcription (Figure S1) but instead may be due to an increase in protein stabilization. Further studies are required to uncover the mechanisms by which these proteins are upregulated.

SERPINS comprise the largest group of protease inhibitors known to date. Despite their functional versatility, all SERPINS contain a highly conserved surface-exposed reactive site loop (RSL), which interacts with the target protease to form tight, irreversible complexes.<sup>9,16</sup> In addition, *SERPINB8* contains two hydrophobic regions in close proximity to the N terminus (Figure 1H), which are thought to be important for secretion of *SERPINB8*; consequently, *SERPINB8* can reside either intracellularly or extracellularly.<sup>17,18</sup> In paraffin-embedded skin sections, *SERPINB8* localizes mainly to the cytoplasm, but the exact epitope to which the antibody binds is unknown. *SERPINB8* signals were strongly reduced in the individual's skin homozygous for c.850C>T (p.Arg284\*). Because the nonsense mutation is located in the last exon of *SERPINB8*, we predict that the transcript will not be subjected to nonsense-mediated mRNA decay, but rather the mutation results in a C-terminally truncated protein. Therefore, the reduced protein levels in the loss-of-function skin suggest that the mutant *SERPINB8* with the alternative C-terminal end is less stable than the wild-type protein. Because we have no access to material from affected individuals of families 1 and 2, we predict the following for the mutations disclosed in those individuals. For the missense variant identified in family 2—c.2T>C (p.Met1?)—which affects the start codon of *SERPINB8*, we postulate the expression of a truncated version of isoform a and full-length isoform c in the affected individual's skin that both lack the two hydrophobic regions and thus, the ability to be transported outside of the cell. Because an additional start codon is present upstream of the RSL, it will most likely be unaffected, and *SERPINB8* is predicted to retain its ability to act as an intracellular protease inhibitor. In contrast, in the frameshift variant, c.947delA (p.Lys316Serfs\*90), identified in the two Tunisian siblings of family 1, the hydrophobic regions will be preserved but the RSL will be fully absent, and the inhibiting properties of *SERPINB8* inside and outside the cell will be completely lost. Even though the type and location of mutations differ in the affected individuals, we predict that all three variants cause *SERPINB8* to lose its ability to act extracellularly. This suggests that *SERPINB8* plays an important role in regulating extracellular protease cascades in skin. In vitro studies have previously found that soluble recombinant furin can be inhibited by *SERPINB8*, presumably by entering the secretory pathway.<sup>18</sup>

Furthermore, we characterized *SERPINB8* in skin and HaCaT human keratinocytes and performed in vitro studies utilizing siRNA-mediated knockdown of *SERPINB8* in keratinocytes. In the absence of *SERPINB8* in keratinocytes, there is a cell-cell adhesion defect, particularly when cells are subjected to mechanical stress, alongside a dysregulation of the desmosomal proteins, desmoplakin, and desmoglein-1. A dysregulation of desmosomal proteins was also reported for the two protease inhibitors, Cystatin A (*CSTA* [MIM: 184600]) and calpastatin (*CAST* [MIM: 114090]), that we have recently implicated in the pathogenesis of peeling skin conditions.<sup>7,8</sup> These similar morphological features associated with loss-of-function mutations in *CSTA* and *CAST* are reflected in some overlap in clinical presentation to individuals harboring homozygous loss-of-function *SERPINB8* mutations. Clinical manifestations related to *CSTA* mutations include palmoplantar keratoderma and superficial exfoliation of the skin (MIM: 607936) whereas mutations in *CAST* underlie generalized skin peeling with underlying erythema, blistering, leukonychia, plantar keratosis, cheilitis, and knuckle pads (MIM: 616295).<sup>7,8</sup>

Interestingly, mutations in *SERPINB7* have recently been identified to cause Nagashima-type palmoplantar keratosis.<sup>3</sup> This study specifically identified the founder mutation c.796C>T (p.Arg266\*) (GenBank: NM\_001040147.2) in the Japanese and Chinese populations, leading to complete loss of the inhibitory activity of *SERPINB7* and significant reduction in protein levels in the lesional skin compared to the control, where *SERPINB7* was located to the cytoplasm of the granular and cornified layer. Similar to *SERPINB8*, *SERPINB7*-related clinical features are confined to distal extremities, particularly on palms and soles, and suggests that both SERPINS are prominent at sites exposed to increased mechanical forces, controlling stress-induced protease cascades.<sup>3</sup> Even though in vitro studies have recently identified several target proteases, including furin, trypsin, and thrombin, the true physiological targets of *SERPINB8* in the skin are still unknown. However, other SERPINS, including *SERPINB3*, *SERPINB4*, and *SERPINB6* that are known to be active in the epidermis, not only effectively inhibit serine proteases, including kallikrein-8 and cathepsin G, but also are capable of inhibiting cysteine proteases like Cathepsin L, Cathepsin K, or Cathepsin S.<sup>2</sup> Together with furin, cathepsins and kallikreins represent the most likely target substrates for *SERPINB8* in skin, because they regulate different stages of keratinocyte differentiation in the epidermis, including cornified envelope formation and desquamation<sup>2</sup> and were also shown to be involved in the processing of desmosomal adhesion molecules.<sup>6,19,20</sup>

In conclusion, we describe mutations in *SERPINB8* that are associated with autosomal-recessive exfoliative ichthyosis and we provide evidence that *SERPINB8* contributes to the mechanical stability of intercellular adhesions in the epidermis. Additional functional assays will be required to investigate the precise physiological

role of SERPINB8 and to unravel its target proteases in the skin.

## Supplemental Data

Supplemental Data include one figure and one table and can be found with this article online at <http://dx.doi.org/10.1016/j.ajhg.2016.06.004>.

## Acknowledgments

We would like to thank the families for their participation in this study. M.P. is supported by a Fellowship from the Deutsche Forschungsgemeinschaft. This work was supported in part by a generous donation of Israel and Ruthi Ram (E.S.) and from a British Heart Foundation Programme grant (D.P.K.).

Received: February 12, 2016

Accepted: June 6, 2016

Published: July 28, 2016

## Web Resources

1000 Genomes, <http://www.1000genomes.org>  
Burrows-Wheeler Aligner, <http://bio-bwa.sourceforge.net/>  
dbSNP, <http://www.ncbi.nlm.nih.gov/projects/SNP/>  
ExAC Browser, <http://exac.broadinstitute.org/>  
GenBank, <http://www.ncbi.nlm.nih.gov/genbank/>  
MultAlin, <http://multalin.toulouse.inra.fr/multalin/>  
MutationTaster, <http://www.mutationtaster.org/>  
NHLBI Exome Sequencing Project (ESP) Exome Variant Server, <http://evs.gs.washington.edu/EVS/>  
OMIM, <http://www.omim.org/>  
ORF Finder, <http://www.ncbi.nlm.nih.gov/gorf/gorf.html>  
PolyPhen-2, <http://genetics.bwh.harvard.edu/pph2/>  
Primer3, <http://bioinfo.ut.ee/primer3>  
SIFT, <http://sift.bii.a-star.edu.sg/>

## References

- de Veer, S.J., Furio, L., Harris, J.M., and Hovnanian, A. (2014). Proteases and proteomics: cutting to the core of human skin pathologies. *Proteomics Clin. Appl.* 8, 389–402.
- de Veer, S.J., Furio, L., Harris, J.M., and Hovnanian, A. (2014). Proteases: common culprits in human skin disorders. *Trends Mol. Med.* 20, 166–178.
- Kubo, A., Shiohama, A., Sasaki, T., Nakabayashi, K., Kawasaki, H., Atsugi, T., Sato, S., Shimizu, A., Mikami, S., Tanizaki, H., et al. (2013). Mutations in SERPINB7, encoding a member of the serine protease inhibitor superfamily, cause Nagashima-type palmoplantar keratosis. *Am. J. Hum. Genet.* 93, 945–956.
- Yin, J., Xu, G., Wang, H., Zhao, J., Duo, L., Cao, X., Tang, Z., Lin, Z., and Yang, Y. (2014). New and recurrent SERPINB7 mutations in seven Chinese patients with Nagashima-type palmoplantar keratosis. *J. Invest. Dermatol.* 134, 2269–2272.
- Sun, L.D., Cheng, H., Wang, Z.X., Zhang, A.P., Wang, P.G., Xu, J.H., Zhu, Q.X., Zhou, H.S., Ellinghaus, E., Zhang, F.R., et al. (2010). Association analyses identify six new psoriasis susceptibility loci in the Chinese population. *Nat. Genet.* 42, 1005–1009.
- Ovaere, P., Lippens, S., Vandenaabeele, P., and Declercq, W. (2009). The emerging roles of serine protease cascades in the epidermis. *Trends Biochem. Sci.* 34, 453–463.
- Blaydon, D.C., Nitoiu, D., Eckl, K.M., Cabral, R.M., Bland, P., Hausser, I., van Heel, D.A., Rajpopat, S., Fischer, J., Oji, V., et al. (2011). Mutations in CSTA, encoding Cystatin A, underlie exfoliative ichthyosis and reveal a role for this protease inhibitor in cell-cell adhesion. *Am. J. Hum. Genet.* 89, 564–571.
- Lin, Z., Zhao, J., Nitoiu, D., Scott, C.A., Plagnol, V., Smith, F.J., Wilson, N.J., Cole, C., Schwartz, M.E., McLean, W.H., et al. (2015). Loss-of-function mutations in CAST cause peeling skin, leukonychia, acral punctate keratoses, cheilitis, and knuckle pads. *Am. J. Hum. Genet.* 96, 440–447.
- Gatto, M., Iaccarino, L., Ghirardello, A., Bassi, N., Pontisso, P., Punzi, L., Shoenfeld, Y., and Doria, A. (2013). Serpins, immunity and autoimmunity: old molecules, new functions. *Clin. Rev. Allergy Immunol.* 45, 267–280.
- Dahlen, J.R., Foster, D.C., and Kisiel, W. (1998). The inhibitory specificity of human proteinase inhibitor 8 is expanded through the use of multiple reactive site residues. *Biochem. Biophys. Res. Commun.* 244, 172–177.
- Li, H., and Durbin, R. (2010). Fast and accurate long-read alignment with Burrows-Wheeler transform. *Bioinformatics* 26, 589–595.
- McKenna, A., Hanna, M., Banks, E., Sivachenko, A., Cibulskis, K., Kernysky, A., Garimella, K., Altshuler, D., Gabriel, S., Daly, M., and DePristo, M.A. (2010). The Genome Analysis Toolkit: a MapReduce framework for analyzing next-generation DNA sequencing data. *Genome Res.* 20, 1297–1303.
- Adzhubei, I.A., Schmidt, S., Peshkin, L., Ramensky, V.E., Gerasimova, A., Bork, P., Kondrashov, A.S., and Sunyaev, S.R. (2010). A method and server for predicting damaging missense mutations. *Nat. Methods* 7, 248–249.
- Kumar, P., Henikoff, S., and Ng, P.C. (2009). Predicting the effects of coding non-synonymous variants on protein function using the SIFT algorithm. *Nat. Protoc.* 4, 1073–1081.
- He, Y., Sonnenwald, T., Sprenger, A., Hansen, U., Dengjel, J., Bruckner-Tuderman, L., Schmidt, G., and Has, C. (2014). RhoA activation by CNFy restores cell-cell adhesion in kindlin-2-deficient keratinocytes. *J. Pathol.* 233, 269–280.
- Heit, C., Jackson, B.C., McAndrews, M., Wright, M.W., Thompson, D.C., Silverman, G.A., Nebert, D.W., and Vasiliou, V. (2013). Update of the human and mouse SERPIN gene superfamily. *Hum. Genomics* 7, 22.
- Dahlen, J.R., Foster, D.C., and Kisiel, W. (1997). Expression, purification, and inhibitory properties of human proteinase inhibitor. *Biochemistry* 36, 14874–14882.
- Dahlen, J.R., Jean, F., Thomas, G., Foster, D.C., and Kisiel, W. (1998). Inhibition of soluble recombinant furin by human proteinase inhibitor 8. *J. Biol. Chem.* 273, 1851–1854.
- Posthaus, H., Dubois, C.M., and Müller, E. (2003). Novel insights into cadherin processing by subtilisin-like convertases. *FEBS Lett.* 536, 203–208.
- Igarashi, S., Takizawa, T., Takizawa, T., Yasuda, Y., Uchiwa, H., Hayashi, S., Brysk, H., Robinson, J.M., Yamamoto, K., Brysk, M.M., and Horikoshi, T. (2004). Cathepsin D, but not cathepsin E, degrades desmosomes during epidermal desquamation. *Br. J. Dermatol.* 151, 355–361.